Balanced-to-unbalanced filtering magic-T based on circular patch resonator with high selectivity

Fei Jiao, Qi Zhang, Qiyun Zhang, Xiang Gao✉, Shuokun Ma and Wanchun Tang

This Letter presents a new design of balanced-to-unbalanced (B2U) filtering magic-T based on circular patch resonator. Without additional circuit, the prescribed in-phase and out-of-phase specifications of the magic-T are achieved by elaborately studying and exploring the electric field distributions of the degenerate resonant modes in the circular patch resonators. Meanwhile, the desired filtering responses are attained by virtue of the coupling extent between the two designed patch resonators in the back-to-back form. In the proposed design, a pair of TM_{11} modes at first make up passband. Meanwhile, nice common-mode suppression can be achieved at the balanced ports, and high isolation is achieved at the single-end ports, respectively. For demonstration, a prototype B2U filtering magic-T working at 4.3 GHz with 3 dB fractional bandwidth of 16.3% is implemented. Measured results coincide well with simulated ones, verifying the proposed design concept.

Introduction: Magic-T and bandpass filters play their important roles in modern wireless communication systems. Integrating the functions of the filter and magic-T into one device will greatly reduce the size of the circuit and improve the overall circuit performance. A filtering magic-T is one kind of filtering coupler, which provides an in-phase/out-of-phase power-division/combination, together with frequency selection function of filter. In recent years, various new types of filtering magic-T have been proposed [1–4]. In order to achieve compact size and improve stopband rejection, four net-type coupled resonators are introduced in the filtering magic-T coupler [1]. By exploring the low-temperature co-fired ceramic technology, a compact filtering magic-T is presented in [2]. To overcome high conductor loss and low power handling capability, substrate integrated waveguide resonators are applied in the design of filtering magic-T as reported in [3, 4]. However, these filtering magic-Ts can only accommodate two integrated functions. It is worth noting that because the balanced circuit can effectively suppress the interference of environmental noise and system electronic noise, it has received more and more attention. In [5], balanced-to-unbalanced (B2U) filtering magic-T is proposed for the first time. It integrates the three functions of filter, magic T and balanced circuit into one device. On the other hand, the patch resonator becomes popular in microwave device designs, attributing to its superiorities of high power handling capacity, low loss and simple circuit layout and so on. For instance, some devices using patch resonators with balanced function have been studied [6, 7]. However, to the best of our knowledge, the B2U filtering magic-T based on the patch resonator has not been reported.

In this Letter, a novel B2U filtering magic-T based on circular patch resonator is presented. To do so, electric field (E-field) distributions of TM_{11} degenerate modes in a circular patch resonator are studied and further explored to achieve the desired 0° and 180° phase differences. By properly arranging the input/output ports and coupling two circular patch resonators in back-to-back form, the B2U filtering magic-T with both good differential-mode (DM) bandpass response and common-mode (CM) suppression is realised. A quarter-wavelength ($\lambda/4$) microstrip open-ended stub is etched in each input/output microstrip feeding transmission line to introduce two transmission zeros (TZs) at both lower- and upper-passband edges, bringing out sharp frequency selectivity. For demonstration, a prototype B2U filtering magic-T is implemented. Both simulated and measured results are in good agreement, which validates the design concept.

Analysis of the circular patch resonator: The circular patch resonator is employed as a basic resonance unit to realise desired responses and phase characteristics for implementation of the proposed B2U filtering magic-T. To do so, the E-field distributions and resonance properties of the circular patch resonator are considered at first. Due to central symmetry of circular patch resonator, the resonant properties of the resonator are investigated and they can be determined by only radius R of such a circular patch resonator. Since the patch resonator can be deemed as a waveguide cavity with magnetic walls along the sides, a similar cavity model theory can be utilised to derive the resonant frequencies of the orthogonal degenerate TM_{11} modes (TM_{11a} and TM_{11b} mode) as [8]

$$f_{nm} = \frac{X_{nm}c}{2\pi R_e\sqrt{\varepsilon_r}}, \quad X_{11} = 1.84118 \tag{1a}$$

$$R_e = R\left[1 + \frac{2h}{\pi R\varepsilon_r}\left(\ln\frac{\pi R}{2h} + 1.7726\right)\right]^{1/2} \tag{1b}$$

where c is the speed of light in free space while ε_r is the relative permittivity of the substrate. By executing full-wave simulation, their resonant frequencies and E-field distributions are investigated. Fig. 1*a* plots E-field of the TM_{11a} mode. As can be seen, the E-field within the patch resonator is classified into two distinctive regions (i.e. regions A and B) in terms of out-of-phase and identical magnitude. Since TM_{11} modes appear as a pair of orthogonal degenerate modes, the E-field property of TM_{11b} is similar to that of TM_{11a} as illustrated in Fig. 1*b*. With the comparison between the two orthogonal degenerate modes, it can be found that the place with strong E-field of TM_{11a} mode exhibits the weak E-field of TM_{11b} mode, or vice versa.

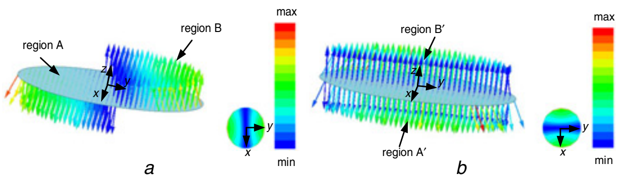

Fig. 1 *E-field distributions of circular patch*
a E-field distributions of TM_{11a} mode
b E-field distributions of TM_{11b} mode

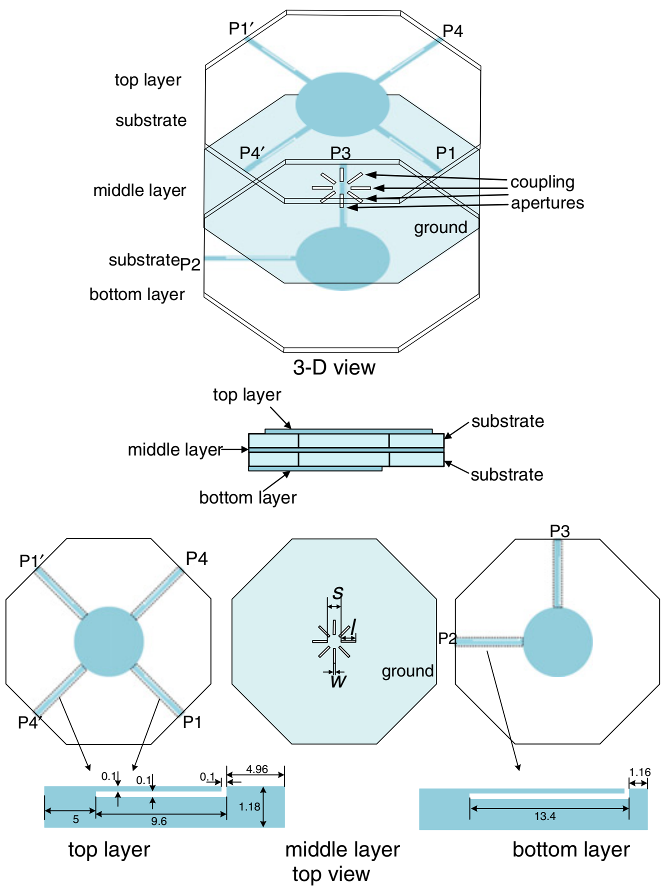

Fig. 2 *Layout of the proposed B2U filtering magic-T*

Design of the proposed B2U filtering magic-T: Fig. 2 shows the designed layout of the proposed B2U filtering magic-T, the proposed structure is designed on a two-layered substrate, where two circular patch resonators are stacked in a back-to-back form and share the common ground plane in the middle layer. Then, eight rectangular coupling apertures are symmetrically etched on the common ground with respect to the centre of these two patches, realising the internal couplings between patch resonators 1 and 2. Two pairs of balanced input ports (P1 and P1′, P4 and P4′) are connected with the top circular patch resonator while the other two single-ended (SE) output ports (P2 and P3) are linked with the bottom patch resonator. In order to excite the orthogonal degenerate modes in each patch resonator, balanced ports (P1 and P1′) and (P4 and P4′) are arranged opposite each other, as shown in Fig. 2. Two SE output ports (P2 and P3) arranged perpendicularly to each other.

Fig. 3 describes the designed coupling topology for the proposed B2U filtering magic-T. In the topology, the white disks $S1$ and $S1'$ ($S2$ and $S2'$) represent a pair of balanced input ports P1 and P1′ (P4 and P4′), while L_1 and L_2 signify the SE output ports P2 and P3, respectively. Besides, each light grey disk represents a circular patch resonator with its degenerate resonant modes. The subscripts a and b denote TM_{11a} and TM_{11b} modes, respectively. Both modes resonate at the same centre frequency of the B2U filtering magic-T.

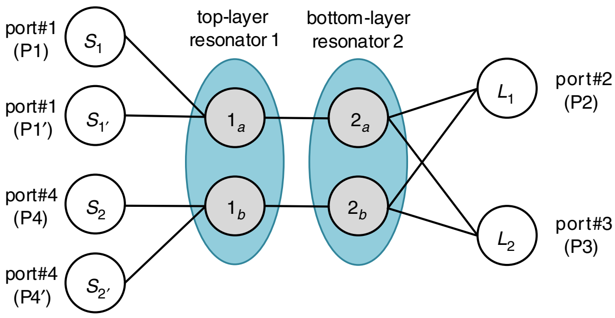

Fig. 3 *Coupling topology of the proposed B2U filtering magic-T*

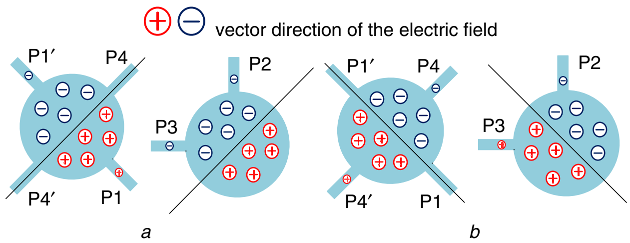

Fig. 4 *E-field distributions of the B2U filtering magic-T*

a When DM signals are injected from P1 and P1′
b When DM signals are injected from P4 and P4′

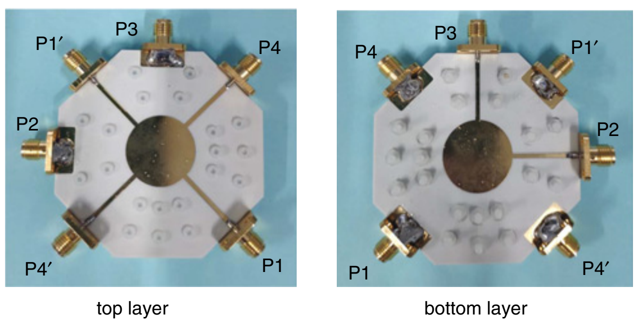

Fig. 5 *Photographs of the fabricated B2U filtering magic-T*

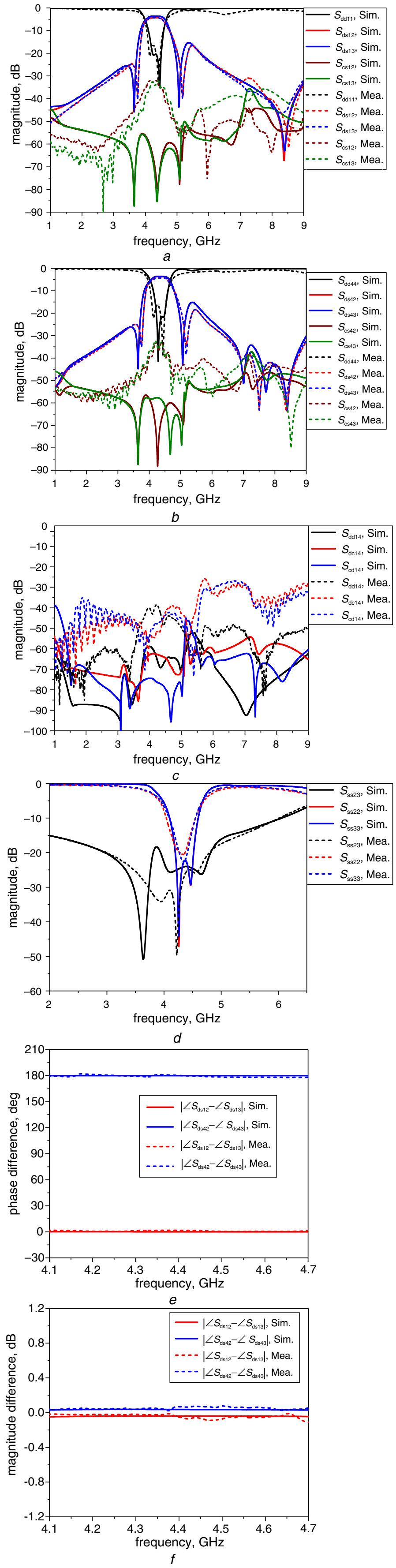

Fig. 6 *Measured and simulated results of the B2U filtering magic-T*

a Magnitudes of S_{dd11}, S_{ds12} and S_{ds13}
b Magnitudes of S_{dd44}, S_{ds42} and S_{ds43}
c Magnitudes of S_{dd14}, S_{dc14} and S_{cd14}
d Magnitudes of S_{ss23}, S_{ss22} and S_{ss33}
e Phase differences between ports 2 and 3
f Magnitude differences between ports 2 and 3

Based on the above topology in Fig. 3, let us consider the transmission properties under DM and CM excitation at the operation frequency. The proposed B2U filtering magic-T is designed to operate at the resonant frequency of TM_{11} mode. According to the analysis of the electric field of the TM_{11} mode in Fig. 1, Fig. 4 further plots the *E*-field directions at the operating frequency when DM signals are injected from different balanced input ports. TM_{11} mode is an odd-order mode with odd symmetrical *E*-field. Therefore, when the balanced input ports (P1 and P1′) are arranged at the relative positions of the left and right sides of the circular patch resonator, the TM_{11a} mode can be well generated in patch resonator 1 under DM excitation. It is worth mentioning that P4 (P4′) is naturally isolated from P1 (P1′) since the *E*-field of TM_{11a} mode is weak at P4 (P4′) and the signal cannot be transmitted from the patch resonator 1 to P4 (P4′). Moreover, through the internal coupling apertures on the common ground, the same field distributions on resonator 1 could be excited on resonator 2, ensuring the in-phase and equal-magnitude signal transmissions to two SE output ports (P2 and P3). On the other hand, when the DM input signal is fed at P4 (P4′), TM_{11b} mode could be excited in patch resonator 1. Similarly, with the introduction of the internal couplings between these two patch resonators, TM_{11b} mode could also be excited on resonator 2, resulting in the out-of-phase and equal-magnitude signal transmissions to output ports P2 and P3, respectively. As for the common mode (CM) excitation, it is apparent that the TM_{11} mode cannot be generated, thus realising good CM suppression. In addition, each input/output microstrip feed line of the B2U filtering magic-T is etched by quarter-wavelength ($\lambda/4$) microstrip open stubs with different lengths to create two TZs at the upper and lower stopband, thus improving the frequency selectivity.

Implementation and results: Based on the above analysis, a prototype B2U filtering magic-T with the centre frequencies of $f = 4.3$ GHz is designed and fabricated for an example. In this design, the substrate is selected as Rogers RO4003C, with a relative permittivity of 3.55, thickness of 0.508 mm and loss tangent of 0.0027. The final optimal layout parameters in Fig. 2 are determined as follows (units: mm): $l = 4.2$, $w = 0.6$, $s = 4$. The radius of the circular patch resonator used in the design is $R = 10$ mm. The photograph of the fabricated B2U filtering magic-T is given in the inset of Fig. 5.

In this work, the simulation and optimisation are carried out via the commercial full-wave simulator HFSS, while the measurement is conducted by using the Agilent N5244A vector network analyser. Fig. 6 shows the simulated and measured results, which coincide well with each other. The subscript *s* is the single-end response, *d* is the DM excitation and *c* is the CM excitation. It is noted in Figs. 6*a* and *b* that two DM *S*-parameters, denoted by S_{dd11} and S_{dd44}, have the same centre frequencies. Their centre frequency are both 4.3 GHz with 3 dB fractional bandwidth of 16.3% while their measured insertion losses are <1.3 dB (excluding the 3 dB division loss) and CM suppressions are higher than 32 dB. Within the passband, the measured return losses (RLs) of the balanced input ports are better than 16.2 dB. Depicted in Fig. 5*c*, the DM isolation between two inputs reach 38 dB and CM isolation is better than 40 dB. Besides, it can be found from Fig. 5*d* that the RLs of SE output ports (P2 and P3) are better than 20 dB, while the isolation between P2 and P3 is higher than 25 dB, thereby indicating good isolation and decent output port matching. The measured in-phase and out-of-phase imbalances are <1.8° and 1.9° inside the passband, respectively, as shown in Fig. 6*e*. The magnitude imbalances for in-phase and out-of-phase operation are <0.09 and 0.08 dB, respectively. In addition, two transmission zeros appear at 3.75 and 5.19 GHz, thereby highly improving frequency selectivity.

Conclusion: This Letter has presented a novel B2U filtering magic-T implemented by using circular patch resonator, for the first time. The proposed B2U filtering magic-T explores the TM_{11} mode of circular patch to achieve good differential mode transmission and CM rejection. A prototype B2U filtering magic-T was implemented to demonstrate the design concept. The results evidently demonstrate that the presented magic-T achieve excellent performances of filtering power division responses, amplitude and phase balance, good DM bandpass response and CM suppression. With these attractive features, it is believed that the proposed circuit is promising in modern wireless communication systems.

Submitted: *11 July 2020* E-first: *2 October 2020*
doi: 10.1049/el.2020.2059
One or more of the Figures in this Letter are available in colour online.
Fei Jiao, Qi Zhang, Qiyun Zhang, Xiang Gao, Shuokun Ma and Wanchun Tang (*School of Electrical and Automation Engineering, Nanjing Normal University, Nanjing 210046, People's Republic of China*)

✉ E-mail: 61188@njnu.edu.cn

References

1 Wang, W., Shen, T., Huang, T.Y., *et al.*: 'Miniaturized rat-race coupler with bandpass response and good stopband rejection'. 2009 IEEE MTT-S Int. Microwave Symp. Digest, Boston, MA, 2009, pp. 709–712
2 Wang, K.X., Liu, X.F., Li, Y.C., *et al.*: 'LTCC filtering rat-race coupler based on eight-line spatially-symmetrical coupled structure', *IEEE Access*, 2018, **6**, pp. 262–269
3 Li, P., Chu, H., and Chen, R.S.: 'SIW magic-T with bandpass response', *Electron. Lett.*, 2015, **51**, (14), pp. 1078–1080
4 Li, H.Y., Xu, J.X., and Zhang, X.Y.: 'Substrate integrated waveguide filtering rat-race coupler based on orthogonal degenerate modes', *IEEE Trans. Microw. Theory Tech.*, 2019, **67**, (1), pp. 140–150
5 Lin, J.Y., Wong, S.Y., Yang, Y., *et al.*: 'Cavity balanced-to-unbalanced magic-T with filtering response'. 2019 IEEE MTT-S Int. Microwave Symp. (IMS), Boston, MA, 2019, pp. 444–447
6 Liu, Q.W., Wang, J.P., Zhang, G., *et al.*: 'A new design approach for balanced bandpass filters on right-angled isosceles triangular patch resonator', *IEEE Microw. Wirel. Compon. Lett.*, 2019, **29**, (1), pp. 5–7
7 Liu, Q.W., Wang, J.P., Zhu, L., *et al.*: 'Design of a new balanced-to-balanced filtering power divider based on square patch resonator', *IEEE Trans. Microw. Theory Tech.*, 2018, **66**, (12), pp. 5280–5289
8 Garg, R., Bhartia, P., Bahl, I., *et al.*: 'Microstrip antenna design handbook' (Artech House, Boston, 2001)